HTML ABSTRACT + LINKS

Resonant and waveguiding defect modes in a two-dimensional electromagnetic band-gap slab structure for millimeter wave frequencies

M. Schuster,[a] O. Antoniuk, P. Lahl, and N. Klein
Institut für Schichten und Grenzflächen (ISG 2) and Center of Nanoelectronic Systems for Information Technology (CNI), Forschungszentrum Jülich, 52425 Jülich, Germany

(Received 2 September 2004; accepted 30 November 2004; published online 28 January 2005)

In this article we report about the investigation of two-dimensional electromagnetic band-gap structures in a slab arrangement for millimeter wave frequencies made from high resistive silicon. We investigated both waveguiding modes of a line defect and resonant modes of a point defect with respect to a possible application as passive elements in millimeter wave integrated circuits. We found that a line defect can act as a broadband waveguide comprising low transmission losses and that localized point defect modes can be excited. In accordance with recent observations at optical frequencies, the quality factor of such a defect mode was found to be affected by the local displacement of certain lattice elements near the point defect. © *2005 American Institute of Physics*. [DOI: 10.1063/1.1851600]

INTRODUCTION

Due to their unique properties,[1] electromagnetic band-gap (EBG) materials are particularly suited for applications as passive elements in high-frequency circuits, such as waveguides with low insertion loss[2,3] and high-Q resonant cavities.[4,5] Beyond their common use for the near-infrared range, the scalability of their properties to arbitrary frequencies allows for possible applications at millimeter wave frequencies, where standard transmission line elements either suffer from high losses (such as planar transmission lines) or cannot be integrated in circuits (such as hollow metal or quasioptical waveguides). It is known for a while that a three-dimensional confinement of electromagnetic waves, as required for circuit integration of passive high-frequency elements, can be achieved in a two-dimensional EBG structure by a combination of Bragg guiding and index guiding.[6–9] This kind of structures can be operated without any metallic part and do therefore not suffer from losses at very high frequencies due to the finite conductivity of the metal. The demonstration of waveguiding and the existence of high-quality factor resonant structures in EBG slab structures for the millimeter wave range are therefore important steps towards the realization of a circuit technology for millimeter and submillimeter waves.

In this paper we report about our investigation on a two-dimensional (2D) EBG structure made from a hexagonal lattice of air holes in a dielectric slab, which possesses a band gap for TE-type modes (modes with their electric field mainly in the plane of periodicity) at frequencies of around 90 GHz. We have investigated its band-gap properties, the transmission behavior of a line defect waveguide, and the existence of point defect modes being excited by the propagating wave in a line defect waveguide. The EBG lattice was machined from a high resistive silicon wafer with a resistivity of $\rho = 8000\ \Omega$ cm, a dielectric constant of $\varepsilon = 11.56$, and a thickness of 525 μm by drilling of a set of air holes forming a hexagonal lattice arrangement. The relative radius of the air holes $r' = r/a$ was chosen to be $r' = 0.3$, which leads to a number of band gaps for TE modes [see Fig. 1(a)]. The dielectric slab is suspended such that an air gap exists above and below the wafer inducing a step in the dielectric constant, which is necessary for index guiding. According to band-gap calculations for this arrangement, a band gap for index guided modes is maximized for a relative height of the slab $h' = h/a$ in the range from 0.5 to 0.8.[6] We have chosen a lattice constant of $a = 1000$ μm, corresponding to a relative slab height of $h' = 0.525$ and a hole radius of $r = 300$ μm. In this case the first band gap for TE modes is located at relative frequencies from $fa/c_{\text{start}} = 0.273$ to $fa/c_{\text{stop}} = 0.352$, corresponding to absolute frequencies from $f_{\text{start}} = 81.9$ GHz up to $f_{\text{stop}} = 105.6$ GHz. The band structure for this arrangement is shown in Fig. 1(b).

FABRICATION

The holes were machined by drilling with a pulsed Nd:YAG (yttrium aluminum garnet) solid-state laser with a power of 150 W, variable pulse length of 0.2–2 μs, and a wavelength of $\lambda = 1024$ nm. A micrograph of the shape and arrangement of the holes can be seen in Fig. 2. It is obvious from Fig. 2(a) that the drilled holes have approximately circular shape. The small steps that can be observed at the edge of the drilled holes are due to the limited step size of the x-y stepper motor of the laser carrier. Nevertheless, the shape of the holes is satisfying. Unfortunately, the backside of the dielectric slab is covered with molten and blown out material that is condensed over the whole surface of the wafer, as shown in Fig. 2(b). It can be assumed that both the thermal stress applied to the material during the drilling of holes and the subsequent condensation of the molten material on the backside of the wafer may cause a considerable performance decrease of the EBG structure.

[a]Author to whom correspondence should be addressed; electronic mail: m.schuster@fz-juelich.de

 © 2005 American Institute of Physics

Downloaded 15 Dec 2006 to 134.94.122.39. Redistribution subject to AIP license or copyright, see http://jap.aip.org/jap/copyright.jsp

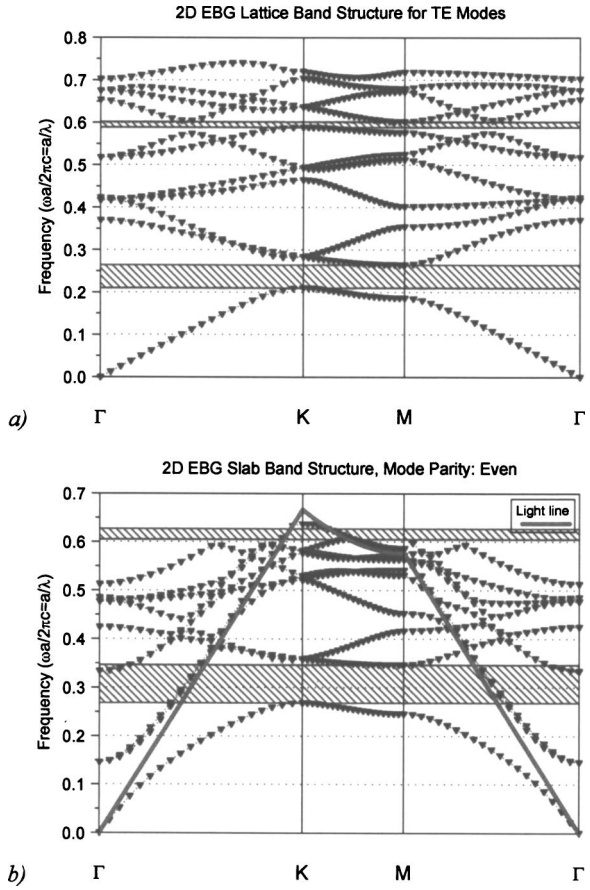


FIG. 1. (a) Calculated band structure for the 2D EBG lattice of air holes in dielectric background material (silicon) with dielectric constant of $\varepsilon = 11.56$ for a relative hole radius of $r' = 0.3$. The structure exhibits a number of band gaps for TE modes. (b) Calculated band structure for even modes in an EBG slab arrangement with a relative height of the slab of $h' = 0.525$, taking into account the dispersion of the cladding material by the introduction of the light line. Three dimensionally confined modes are located in the regions of the band gaps that lie below the light cone.

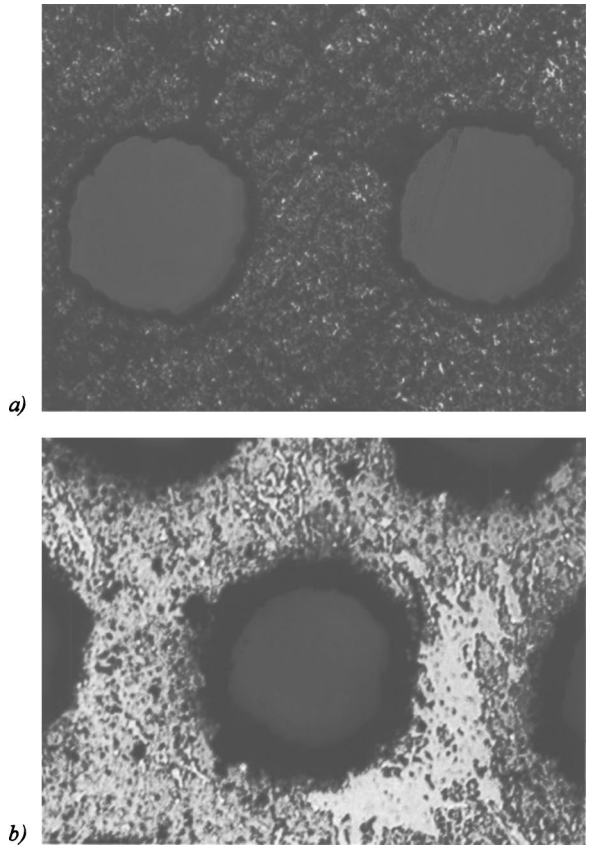


FIG. 2. (a) Micrograph of two adjacent holes of the 2D EBG structure made by laser machining. The shape of the holes is approximately circular. Distortions from the circular shape arise from the limited step size of the laser stepper motor. (b) The backside of the slab is soiled due to the thermal stress during the fabrication process and the deposition of molten material on this surface.

MEASUREMENT SETUP

We have measured the absolute values of transmitted power through the sample employing continuous-wave signals generated by two heterodyne multipliers (Millitech FEX 10-1, FEX 10-6) covering a frequency range from 70 to 90 GHz and from 90 to 110 GHz, respectively. The multipliers were fed with a microwave signal from a synthesized sweeper (HP 83630-A) that delivers frequencies from 10 MHz up to 26.5 GHz. The millimeter wave signal was guided into the EBG structure by a standard rectangular metal waveguide for the WR-10 frequency band with a cross section of 2.5×1.25 mm^2. The EBG structure under investigation was connected to the waveguide by inserting a triangular-shaped taper structure into the waveguide in order to provide a smooth transition between the rectangular metal waveguide filled with air and the silicon slab in which the EBG structure was patterned, and to minimize the reflection of the wave at the air-dielectric boundary. The transmitted signal was coupled into a rectangular waveguide with a similar taper and subsequently fed into a Schottky detector diode (Millitech DXP-10 for frequencies from 75 to 110 GHz). The experimental setup is shown in Fig. 3. Two isolators were used to prohibit the backward propagation of a reflected signal into the source and detectors, as seen in Fig. 3. The transmission coefficient was determined as ratio of transmitted power with and without sample. For the latter the waveguide ports were connected with screws. The experimental results were compared with three-dimensional (3D) field simulation of the waveguide EBG assembly employing a commercial time domain finite integration technique solver (CST Microwave Studio).

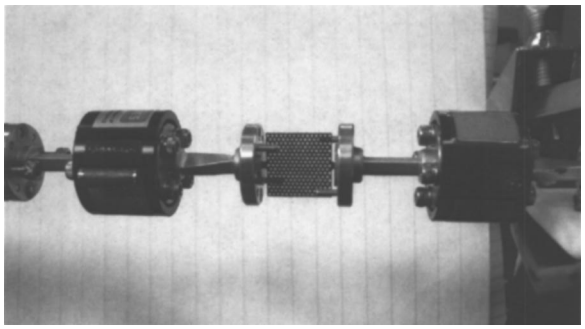


FIG. 3. Experimental setup: the patterned silicon structure was clamped between two rectangular waveguide ports, the signal source was connected on the left side, and the detector diode was connected on the other side. Two isolators were used to prevent standing wave effects from reflections at the interfaces and diodes.

Downloaded 15 Dec 2006 to 134.94.122.39. Redistribution subject to AIP license or copyright, see http://jap.aip.org/jap/copyright.jsp

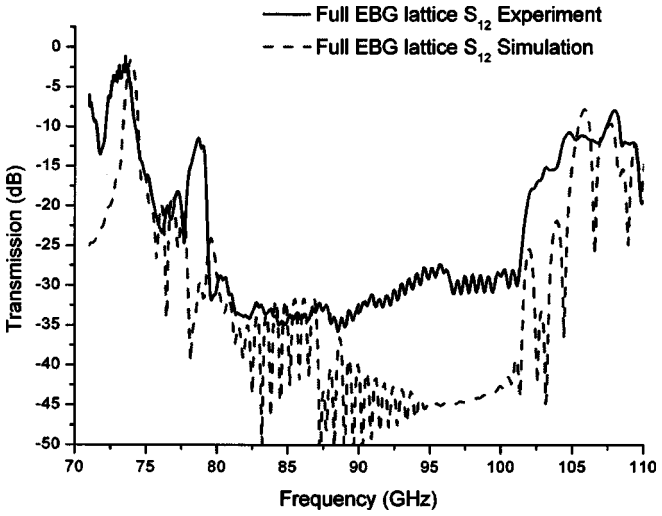


FIG. 4. Comparison between experimental curve and simulation for the full EBG lattice without defects. The frequency range for which there is a transmission drop due to the band gap of the structure in good agreement in both curves.

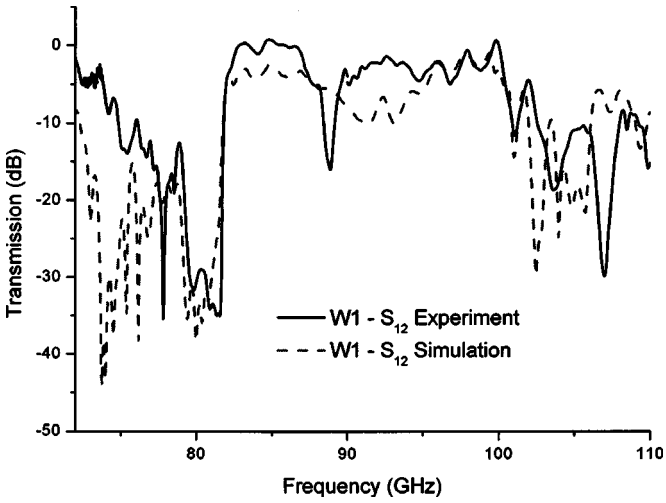


FIG. 5. Comparison between experimental curve and simulation for the EBG structure with a W1 line defect waveguide. For the frequency range between 82 and about 97 GHz, the line defect acts as a waveguide with high transmission between −1 and −6 dB.

EXPERIMENTAL RESULTS

The first measurement was done to confirm the existence of the band gap and investigate the strength of the coupling between the metal waveguide and the EBG structure. Also, the influence of positioning the structure inside the waveguide had to be investigated, as it was done manually. The measurement was performed with an EBG structure without defects such that a transmission drop for frequencies in the band gap is expected. A comparison between the experimental and simulation results is shown in Fig. 4, and it is observed that both curves are in relatively good agreement considering the frequencies and depth of the transmission drop due to the band gap. For frequencies outside the band gap, the measured insertion loss of about 5–10 dB may be related to the nonoptimized coupling from the rectangular waveguide to the dielectric structure. At frequencies of about 80 and 105 GHz, the falling and rising slopes due to the band gap can be observed. These frequencies coincide nicely with the frequency of the band gap of 81.9 and 105.6 GHz as expected from the simulation. Inside the band gap the transmission is reduced by about 25 dB relative to frequencies outside the band gap, and no spectral features are observed, apart from a very small standing wave pattern, as expected in accordance with the simulation results. In order to investigate the precision of placement of the structure within the waveguide, we have removed the sample from the setup and put it back again. A second measurement of the curve yielded only very slight changes to the transmission curve, thus it is assured, that a manual placement of the EBG structure in the measurement setup is appropriate.

LINE DEFECT WAVEGUIDING

It has been reported before that for microwave frequencies under certain conditions a line defect can have an in-gap cutoff defect frequency $f_{c,d}$ and shows a reasonable transmission behavior for frequencies $f > f_{c,d}$, but no transmission for $f < f_{c,d}$.[2] This type of line defect, where one row of lattice elements is removed (W1 line defect), has the potential to act as a broadband transmission line element. We have measured the W1 line defect structure to confirm these findings at millimeter wave frequencies. Figure 5 shows the comparison between the measurement and simulation for the transmission parameter of the EBG structure with a W1 line defect. The onset of the band gap at frequencies around 80 GHz can be recognized by a transmission drop of about 30 dB for frequencies $f > f_{\text{start}}$, $f < f_{c,d}$. When the cutoff frequency of the defect waveguide is reached at a frequency around 82 GHz, the transmission rises to a level of about −3 dB and,

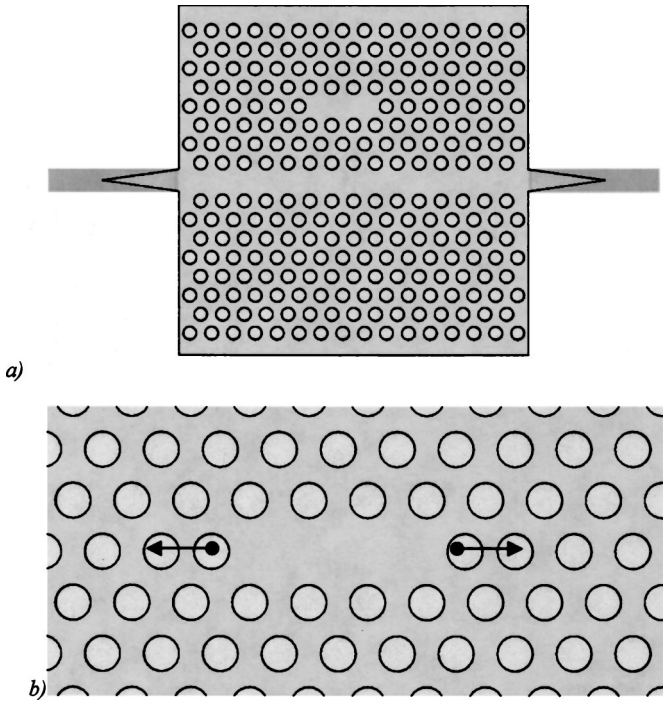


FIG. 6. (a) Transmission measurement setup for a resonant point defect in band reject arrangement. The signal passed through the line defect waveguide and is coupled into the defect for the defect mode resonance frequencies. (b) Displacement of the adjacent lattice holes away from the defect.

Downloaded 15 Dec 2006 to 134.94.122.39. Redistribution subject to AIP license or copyright, see http://jap.aip.org/jap/copyright.jsp

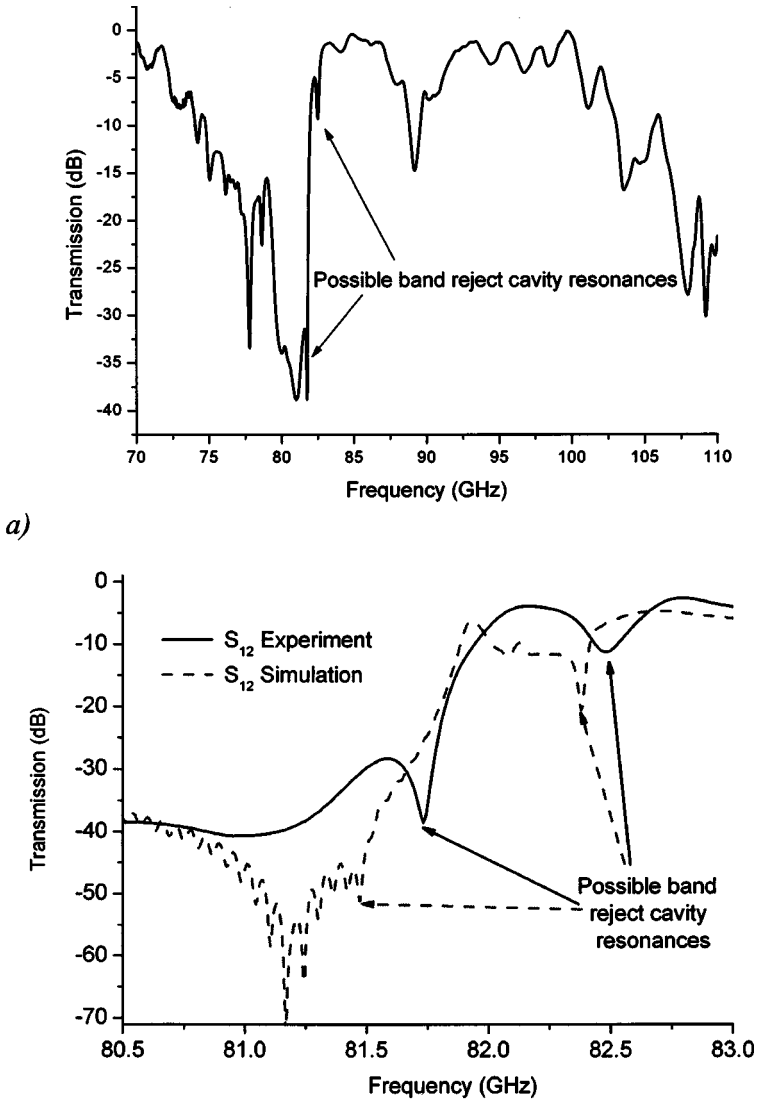


FIG. 7. (a) Measured transmission curve of the resonant point defect in band reject configuration. The curve is very similar to the transmission curve for the W1 waveguide, however, small dips indicate the possible existence of band reject defect resonances. (b) Close view of the transmission dips possibly related to band reject defect resonances.

apart from a minor standing wave pattern that arises from reflections between the waveguide flanges, there is a broadband high transmission region for this waveguide with insertion loss values between −0.5 and −3.5 dB for frequencies from 82 up to 99 GHz. The transmission drop by almost 20 dB at a frequency of 88.7 GHz can currently not be explained. It is not a feature of the band-gap structure, because it exists consistently in all our measurements independent of the structure being measured, but cannot be reproduced by simulation. Therefore, we assume an influence of the measurement setup that so far could not be eliminated. With this measurement it was demonstrated that the W1 waveguide can act as a transmission line for millimeter waves very similar to what we have found for the microwave range before for TM band-gap structures.[2] We expect a further reduction of the insertion loss by optimized impedance matching between the metal waveguide and the W1 line defect. In the following we describe the excitation of defect resonances by the W1 waveguide.

POINT DEFECT RESONATORS

We have investigated the possibility of utilizing a point defect in the EBG lattice as an integrated resonator that can support a localized defect mode with a potentially high-quality factor. Therefore, we have investigated a band reject (notch) resonator very similar to a structure that was investigated at optical frequencies.[10,11] The setup is shown schematically in Fig. 6(a). For a band reject resonator the signal is coupled from the waveguide into the point defect such that the transmission through the waveguide is decreased at its resonance frequencies. Therefore, we expect a dip in the transmission curve. It has been reported in the literature that a defect resonator embedded in a 2D EBG slab exhibits extremely high-quality factors if the holes adjacent to the point defect are displaced from their positions by a few percent of the lattice constant[10,11] (see Fig. 6(b) for a schematic drawing of the displacement). These findings were made at optical frequencies, however, we have investigated a similar structure at a frequency of 90 GHz aiming towards the construction of an integrated high-Q resonator for millimeter wave frequencies. The measured transmission curve of our band reject resonator is shown in Fig. 7(a). The transmission curve in this configuration is very similar to the one already observed for the W1 waveguide. The influence of the point defect can be seen from small transmission dips at frequen-

Downloaded 15 Dec 2006 to 134.94.122.39. Redistribution subject to AIP license or copyright, see http://jap.aip.org/jap/copyright.jsp

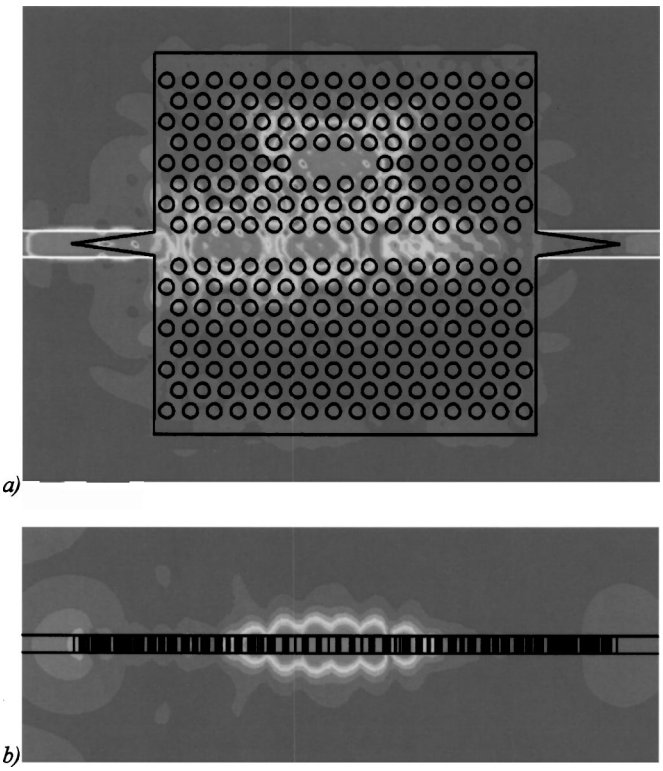


FIG. 8. (a) Simulated distribution of the electric-field amplitude for the resonance frequency at $f_{2,\mathrm{Sim}}=82.38$ GHz. The dip that is found at this frequency is related to a defect mode and energy is coupled from the W1 waveguide into the defect. (b) From the lower picture it becomes clear that the mode is nicely confined to the plane of the 2D EBG slab and radiation is not significant.

cies of $f_1=81.74$ GHz and $f_2=82.47$ GHz which have been marked with arrows in Fig. 7(a). For a clarification of the situation, the transmission curve around these dips is plotted with higher resolution [Fig. 7(b)] from both the experiment and simulation. The existence of the dips could be confirmed by the simulation, and their experimentally measured resonance frequencies can be reproduced if the dielectric constant of the material is used as a parameter in the simulations. A coincidence is found for a dielectric constant of $\varepsilon=11.78$, which is in good agreement with the expected value of 11.56 as used in our previous calculations, taking into account possible degradations of the material during the fabrication process. In this case, the simulated frequencies of the dips are $f_{1,\mathrm{Sim}}=81.46$ GHz and $f_{2,\mathrm{Sim}}=82.38$ GHz, which is in relatively good coincidence with the experimentally found values. However, when the distribution of the electric field at the frequencies of the dips is calculated, it becomes obvious that only one of them is related to the excitation of a localized point defect mode. The electric-field distribution for this peak with the experimental resonant frequency of $f_2=82.47$ GHz is shown in Fig. 8. One can see that the field energy is strongly confined to the position of the defect due to Bragg reflection by the 2D EBG lattice [Fig. 8(a)] and the index guiding [Fig. 8(b)]. For the peak at a lower experimental frequency of $f_1=81.74$ GHz, the calculated field distribution indicates that it corresponds to a surface mode of the EBG lattice that has its field maxima at the side edges of the wafer. It is associated to the point defect because the distance

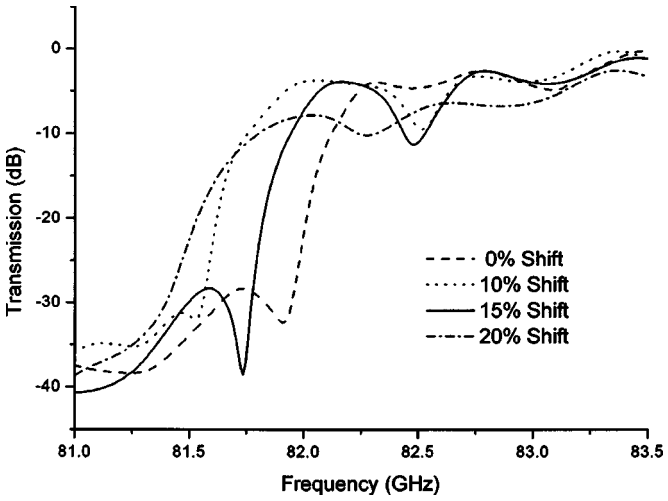


FIG. 9. Comparison of the transmission curves for band reject point defects, where the first holes of the lattice are displaced by a fraction of the lattice constant. Both the resonant frequency and the depth of the dip are strongly dependent on the displacement.

between the upper edge of the structure and the point defect is relatively small (four lattice periods), but the amount of energy of this mode that is stored in the volume of the point defect is rather small. We can assume that this mode would correspond to a resonant mode of the defect, but it is not possible to couple to the mode because its frequency is located at the very beginning of the slope related to the cutoff of the defect waveguide. Therefore, energy cannot be transferred to the defect through the waveguide.

A second indication that the observed dips are related to the defect modes is due to the observation of the influence of the displacement of the lattice elements on the Q factor and the frequency of the resonant mode, given by the half-width and position of the dip. We have measured a number of structures with different displacements of these holes. The comparison of the experimental curves for the frequency range of interest (80–86 GHz) is shown in Fig. 9. It is observed that for displacement of 10% and 15% of the lattice constant the transmission dips are most clearly pronounced. For both 0% and 20% displacements the dips are broader and less deep. This result agrees with the findings that have been reported in the literature.[10,11] We have calculated the unloaded quality factor of the resonant mode from its center frequency f_0, its depth $|S_{21}|$ on a linear scale and its half-width Δf

$$Q_0=\frac{f_0}{\Delta f}\frac{1}{|S_{12}|}. \tag{1}$$

In Table I the resonance frequencies and unloaded quality factors for the defect mode for different displacements of the holes are compared. Similar to the findings reported in the literature, the quality factor is relatively high for displacements of 10% and 15%, while it is reasonably lower for displacements of 0% and 20%. The dependence of the quality factor on the displacement of the holes can be explained, when the Fourier transform of the electric-field distribution is calculated and compared with the region of radiative modes with small k vectors that are able to couple to the

Downloaded 15 Dec 2006 to 134.94.122.39. Redistribution subject to AIP license or copyright, see http://jap.aip.org/jap/copyright.jsp

TABLE I. Measurement of resonant frequency and unloaded quality factor of the resonant mode of the defect according to the field distribution shown in Fig. 8. For different displacements of lattice elements both values are changed and displacements of 10% and 15% yield a large quality factor.

Displacement (% of lattice constant *a*)	Mode frequency (GHz)	Mode quality factor
0	82.478	290
10	82.519	760
15	82.478	700
20	82.273	350

continuum of modes above and below the slab. A more precise explanation is given in the literature and will not be further discussed here.[11] From the material properties of the silicon used for the construction of the EBG slab, we can estimate a maximum quality factor

$$Q \geqslant \frac{1}{\tan \delta} = \frac{\varepsilon_0 \varepsilon \omega}{\sigma} = \varepsilon_0 \varepsilon \omega \rho \tag{2}$$

which is related to its resistivity. In our case, we can expect a maximum quality factor of about 6500. Unfortunately, the experimental findings differ by about one order of magnitude. This decreased quality factor may be explained by the bad condition of the sample surface, as explained before. Additionally, it can be assumed that amorphous regions near the drilled holes were formed during the treatment with the laser beam, which may lead to a significantly lower-quality factor. For a more detailed analysis of the dependence of the achievable quality factors on the surface, more careful investigation of alternative polishing methods, that also involve chemical polishing is necessary. Additionally, alternative drilling methods, such as ultrasonic drilling or water beam drilling, should be investigated to avoid a possible degradation of the silicon during the fabrication process. Alternatively, high aspect ratio silicon etching could be a suitable alternative.[12]

CONCLUSION

It was shown that a 2D EBG slab structure made by simple laser drilling can provide a band gap for TE type modes at frequencies around 90 GHz, and low loss waveguiding for a broad frequency range of more than 20 GHz by a line defect is possible. A three-dimensional confinement of both the traveling line defect mode and a localized point defect mode could be demonstrated. It has also been shown that it is possible to couple energy propagating through a line defect into a resonant point defect and to tune the quality factor of the defect mode by a displacement in the position of adjacent lattice elements. These results show that EBG structures are very well suited for the development of an integrated circuit technology based on 2D EBG slab structures with both Bragg and index guiding for the frequencies in the millimeter wave range.

[1] J. D. Joannopoulos, R. D. Meade, and J. N. Winn, *Photonic Crystals* (Princeton University Press, Princeton, NJ, 1995).
[2] M. Schuster and N. Klein, J. Appl. Phys. **93**, 3182 (2003).
[3] R. Biswas, Z. Y. Li, and K. M. Ho, Appl. Phys. Lett. **84**, 1254 (2004).
[4] T. Yoshie, J. Vuckovic, and A. Scherer, Appl. Phys. Lett. **79**, 4289 (2001).
[5] Z. Zhang and M. Qiu, Opt. Express **12**, 3988 (2004).
[6] S. Johnson, S. Fan, P. R. Villeneuve, J. D. Joannopoulos, and L. A. Kolodziejski, Phys. Rev. B **60**, 5751 (1999).
[7] E. Chow *et al.*, Nature (London) **407**, 983 (2000).
[8] S. Johnson, P. R. Villeneuve, S. Fan, and J. D. Joannopoulos, Phys. Rev. B **62**, 8212 (2000).
[9] T. Sondergaard and A. Lavrinenko, Opt. Commun. **203**, 263 (2002).
[10] Y. Akahane, M. Mochizuki, T. Asano, Y. Tanaka, and S. Noda, Appl. Phys. Lett. **82**, 1341 (2003).
[11] Y. Akahane, T. Asano, B. S. Song, and S. Noda, Nature (London) **425**, 944 (2003).
[12] M. Schuster, N. Klein, P. Ruther, A. Trautmann, O. Paul, P. Kuzel, and F. Kadlec (unpublished).

Downloaded 15 Dec 2006 to 134.94.122.39. Redistribution subject to AIP license or copyright, see http://jap.aip.org/jap/copyright.jsp